Journal of Chromatography, 439 (1988) 137–149
Elsevier Science Publishers B.V., Amsterdam — Printed in The Netherlands

CHROM. 20 353

SINGLE-COLUMN ANION CHROMATOGRAPHY WITH INDIRECT UV DETECTION USING PYROMELLITATE BUFFERS AS ELUENTS

A. JARDY*, M. CAUDE, A. DIOP, C. CURVALE and R. ROSSET
Laboratoire de Chimie Analytique, Ecole Supérieure de Physique et de Chimie de Paris, 10 rue Vauquelin, 75231 Paris Cedex 05 (France)

SUMMARY

Ion chromatography can be conveniently carried out with conventional high-performance liquid chromatographic equipment and classical ion exchangers using a single column and a UV-absorbing eluent ion. Solute peaks are detected as vacancy peaks (corresponding to a decrease in eluent absorbance).

Benzenepolycarboxylate buffers such as those obtained from pyromellitic acid are used as eluents for anion analysis; owing to the four carboxylic acid groups, the eluent ion charge varies with pH, and the eluting power can be adjusted within a wide range. A linear relationship holds between the logarithm of the solute capacity factor and the logarithm of the concentration of the eluting species; the slope observed is $-x/y$, here x and y are the charges on the solute and eluent anion, respectively. At a constant analysis time, the best sensitivity is achieved when the initial absorbance of the eluent (determined by the detection wavelength) is high but its concentration is low, and therefore its charge is high enough to give the required eluting power. Within the linearity range, quantitative analysis requires only one calibration graph when peak-area measurements are performed. The detection limits are about 2–5 ng injected and compare favourably with other detection modes, considering the simplicity of the method. Various examples of separations of inorganic and organic anions are given.

INTRODUCTION

Although it is a young technique, ion chromatography is now being used routinely in a growing number of fields[1–4]. Since its introduction by Small *et al.* in 1975[5] and the development of noteworthy improvements in suppressed ion chromatography[6–9], several alternative methods have been developped to avoid the eluent suppression step. These methods, termed "single-column ion chromatography", use either the conductometric detection directly on the effluent from the separation column or other detection modes, such as UV absorbance, refractive index or electrochemical measurements[10–13]. Some of these can be employed in the direct or indirect detection mode.

0021-9673/88/$03.50

We were interested in a method using conventional high-performance liquid chromatographic (HPLC) equipment. Our study was confined to anion analysis, because of the paucity of analytical procedures for these species. Two problems, which are closely related, have to be solved in anion chromatography: the separation and the detection of a wide range of anions, mainly inorganic but also some organic. In consideration of our objectives, we chose ion exchange for the separation and indirect UV absorption, also called "vacancy detection", for detection. In this paper, the results obtained with pyromellitate buffers as eluents are described. We show how the mobile phase composition, *i.e.*, the concentration and pH of the buffer, can rationally be selected to produce a good separation in a convenient time and with sensitive detection.

THEORY

For a solute anion S^- and an eluent anion E^- the following ion-exchange equilibrium applies:

$$S_S^- + E_M^- \rightleftharpoons S_M^- + E_S^-$$

where the subscripts M and S refer to the mobile and stationary phase, respectively. The ion concentration profiles during the elution of S^- by E^- are shown in Fig. 1. Two peaks can be observed for E^-: the first corresponds to the solute fixation, leading to the displacement of an equivalent amount of E^-; the second, in the opposite direction, corresponds to the default in E^- when the solute band emerges from the column. The latter vacancy peak is the reversed image of the solute peak (S^-). When using an eluent that absorbs strongly at the detection wavelength, this vacancy peak can be used to visualize the elution of a solute that is transparent at this wavelength. Coupling anion-exchange chromatography and indirect UV absorbance leads to contradictory requirements resulting from the separation and the detection. First, for the separa-

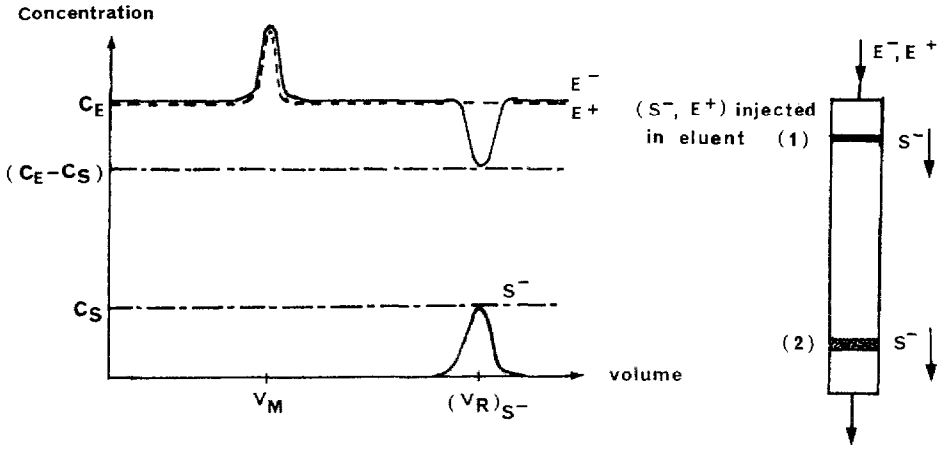

Fig. 1. Concentration profiles during the elution of solute E^+S^- by eluent E^+E^-. (1) Band of S^- at the beginning of the elution (S^- fixation) which gives the E^- peak. (2) S^- band at the end of the elution. The S^- peak corresponds to a decrease in E^- concentration in the effluent. Solid line, E^-; broken line, E^+.

tion, it is necessary to achieve a satisfactory resolution in a convenient time. Consequently, the column must contain a large number of theoretical plates and have a good mass transfer to permit the optimization of the analysis time. The capacity of the ion exchanger has to be neither too low, to avoid column overloading by major constituents in the trace analysis of real samples, nor too high, to permit the use of sufficiently diluted eluents.

However, if the exchanger capacity is higher than usual in single-column ion chromatography, the eluent must have a high eluting power, particularly when its concentration has to be limited to the millimolar range or less, owing to the detection mode. As a result, its charge should be high (the higher the charge, the stronger is the affinity for the resin).

From the detection point of view, the eluent should provide a high sensitivity, good universality and easy quantitation. The first two conditions are fulfilled if the eluent absorbs strongly at the detection wavelength, whereas the sample ions are transparent at this wavelength. The third condition implies that the absorbance measurements are made in the validity range of the Lambert–Beer law, *i.e.*, the initial absorbance and hence concentration are not too high.

Choice of the eluting ion

Buffers prepared from pyromellitic acid (1,2,4,5-benzenetetracarboxylic acid) are convenient eluents: first, they absorb strongly in the UV region owing to their aromatic ring, at wavelengths where most inorganic ions do not, and second, owing to the four carboxylic groups, the charge on the driving ion varies up to 4 depending on the pH. Because the pK values are close to each other, the apparent charge, defined as

$$y = \frac{4\,[E^{4-}] + 3\,[HE^{3-}] + 2\,[H_2E^{2-}] + [H_3E^{-}]}{[E^{4-}] + [HE^{3-}] + [H_2E^{2-}] + [H_3E^{-}] + [H_4E]}$$

(where [ ] refer to the concentrations of the different forms of the acid symbolized as H_4E) varies continuously as a function of pH (Fig. 2).

Detection optimization

Considering the elution of the sample ion S^{x-} by the eluent ion E^{y-}, where y is the apparent charge, the anion-exchange equilibrium can be represented by the equation

$$x\,E_S^{y-} + y\,S_M^{x-} \rightleftharpoons x\,E_M^{y-} + y\,S_S^{x-} \qquad (1)$$

The solute capacity factor can be expressed by the well known relationship[14–16]

$$k'_S = \frac{m}{V_m}(K_E^S)^{1/y}\left(\frac{Q}{[E^{y-}]_0}\right)^{x/y} \qquad (2)$$

where m = mass of resin in the column, V_m = volume of mobile phase inside the

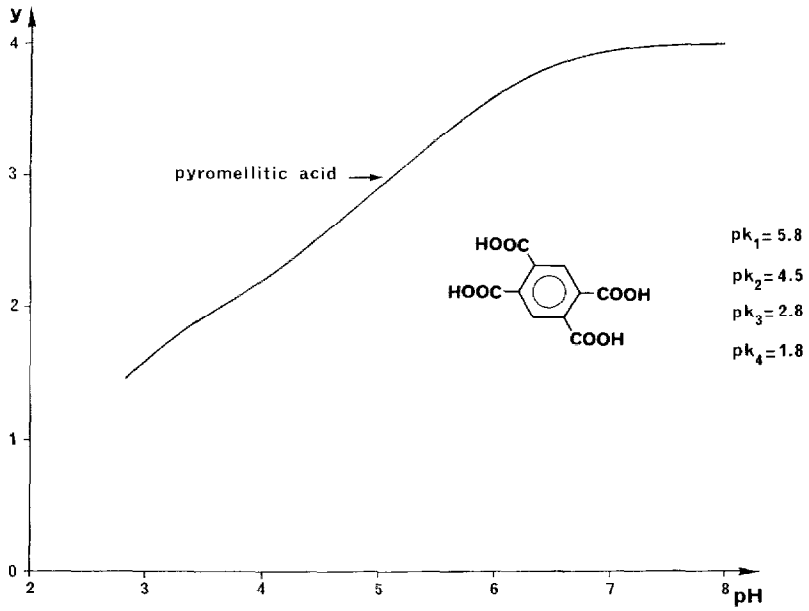

Fig. 2. Variation of the apparent charge, y, of pyromellitic acid *versus* pH (obtained by a microcomputer simulation, using the TOT program[21]).

column, K_E^S = exchange constant between S^{x-} and E^{y-}, Q = capacity of the exchanger and $[E^{y-}]_0$ = total concentration of buffer.

As usual in ion chromatography, concentrations were used in the calculations instead of ion activities, which are really involved in the thermodynamic exchange constant. This classical approximation, for the sake of simplicity, relies on the fact that both the solute end eluent concentrations are low, owing to the analytical conditions and the low ion exchange capacity.

It must be pointed out that for a given column (where m, V_m and Q are constants), isocapacitive eluents can be obtained in several ways: more concentrated but less charged or *vice versa*. In all instances their composition must satisfy the relationship

$$\frac{K_E^S}{([E^{y-}]_0)^x} = \text{constant}$$

The change, ΔC, in the concentration of E^{y-} during the elution of S^{x-}:

$$\Delta C = [E^{y-}] - [E^{y-}]_0$$

can be calculated according to the charge balance:

$$x\,[S^{x-}] + y\,[E^{y-}] = y\,[E^{y-}]_0$$

and is equal to

$$\Delta C = \frac{x}{y}[S^{x-}] \tag{3}$$

Consequently, according to the Lambert–Beer law, the peak absorbance (*i.e.*, change in the effluent absorbance, ΔA) is given by

$$\Delta A = l(\varepsilon_S^\lambda - \frac{x}{y}\varepsilon_E^\lambda)\,[S^{x-}]$$

where ε_S^λ and ε_E^λ are the molar absorptivities of the solute and the eluent at the detection wavelength, respectively, and l is the cell path length. If now $\varepsilon_S^\lambda = 0$ (solute transparent at λ), then

$$\Delta A = -\frac{x}{y}\,\varepsilon_E^\lambda\, l\,[S^{x-}] \tag{4}$$

Eqn. 4 shows that the absorbance decrease varies as the ratio ε_E^λ/y. From the detection point of view, the higher the molar absorptivity of the eluent and the lower its charge, the better is the sensitivity. However, a compromise has to be found in order to have an acceptable eluting power.

Quantitative analysis

Either peak height or peak area can be measured. The latter is generally considered to be more precise, for well resolved peaks, under isocratic conditions[17].

The peak height, h, is proportional to the absorbance decrease:

$$|h| = \alpha\, l\,\frac{x}{y}\,\varepsilon_E^\lambda\,[S^{x-}]_{max} \tag{5}$$

where $[S^{x-}]_{max}$ is the maximum concentration of the solute and α a proportionality constant. Hence $|h|$ increases with increase in the ratio ε_E^λ/y, and depends on the dilution factor due to the column.

With regard to peak area, given by

$$a = \alpha \int |\Delta A|\, dt$$

According to eqn. 4,

$$a = \alpha \cdot \frac{x}{y} \cdot \varepsilon_E^\lambda \cdot l \int [S^{x-}]\, dt$$

$$a = \alpha \cdot \frac{x}{y} \cdot \varepsilon_E^\lambda \cdot l \cdot \frac{q_S}{D} \tag{6}$$

where D is the flow-rate and q_S the amount of solute injected.

Indirect UV absorption has the major advantage of providing the same equivalent response for all sample ions that are transparent at the detection wavelength. Whereas peak-height measurements require a calibration graph for each solute, owing to differences in retention characteristics, peak-area measurements need only one

(for same amount injected, the peak area observed with a solute bearing $2x$ charges will be twice that observed with a solute bearing x charges).

EXPERIMENTAL

Instrumentation

The liquid chromatograph was a Varian (Palo Alto, CA, U.S.A.) Model 5010 instrument equipped with a Shimadzu Model SPD-6A variable-wavelength detector and a Shimadzu Model CR3A integrator (Touzart et Matignon, Vitry-sur-Seine, France).

A Hamilton PRP X-100 poly(styrene–divinylbenzene)-based anion-exchange column (150 × 4.1 mm I.D.) and a Chrompack Ionospher A silica-based anion-exchange column (250 × 4.8 mm I.D.) were used and the temperature was set at 25°C.

Reagents

All solutions were prepared in doubly distilled, deionized water by dissolution of analytical-reagent grade chemicals.

Eluents were prepared from pyromellitic acid (Merck, Darmstadt, F.R.G.), and sodium hydroxide. Sample solutions were obtained from stock solutions, by dilution with eluent, and were injected on to the column using a 20- or 100-μl sample loop injector. Other relevant operating conditions are given in the figure captions.

RESULTS AND DISCUSSION

Retention behaviour of anions versus eluent strength

Fig. 3 shows the variation of the capacity factors of Br^-, NO_3^-, SO_4^{2-} *vs.* eluent

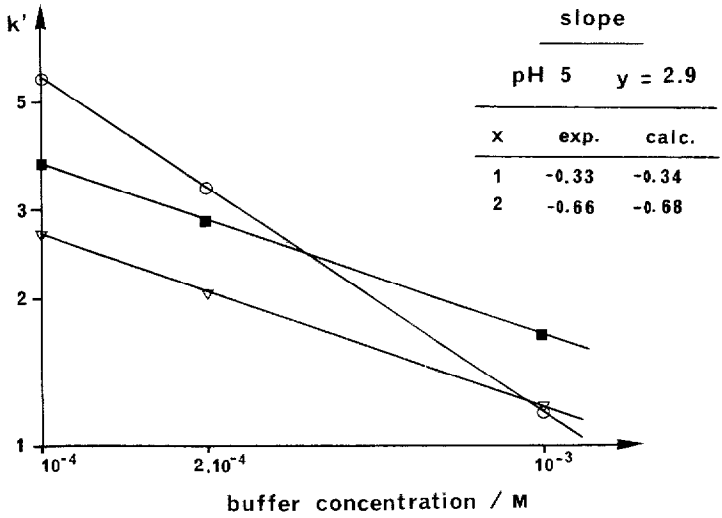

Fig. 3. Variation of solute capacity factors *versus* buffer concentration (logarithmic coordinates). Column, 150 × 4.1 mm I.D.; stationary phase, PRP X-100 (Hamilton); eluent, pyromellitate buffer (pH 5); flow-rate, 1 ml min^{-1}. Solutes: ○, SO_4^{2-} ; ■, NO_3^- ; ▽, Br^-.

concentration, in logarithmic coordinates, for a pH value where the apparent charge on the eluting ion is 2.9. As predicted by eqn. 2, the plots are linear. Moreover, the slopes observed in practice are in excellent agreement with the theoretical values predicted from eqn. 2, for both divalent anions (SO_4^{2-}) and univalent anions (Br^- and NO_3^-). The same results were observed at different pH values.

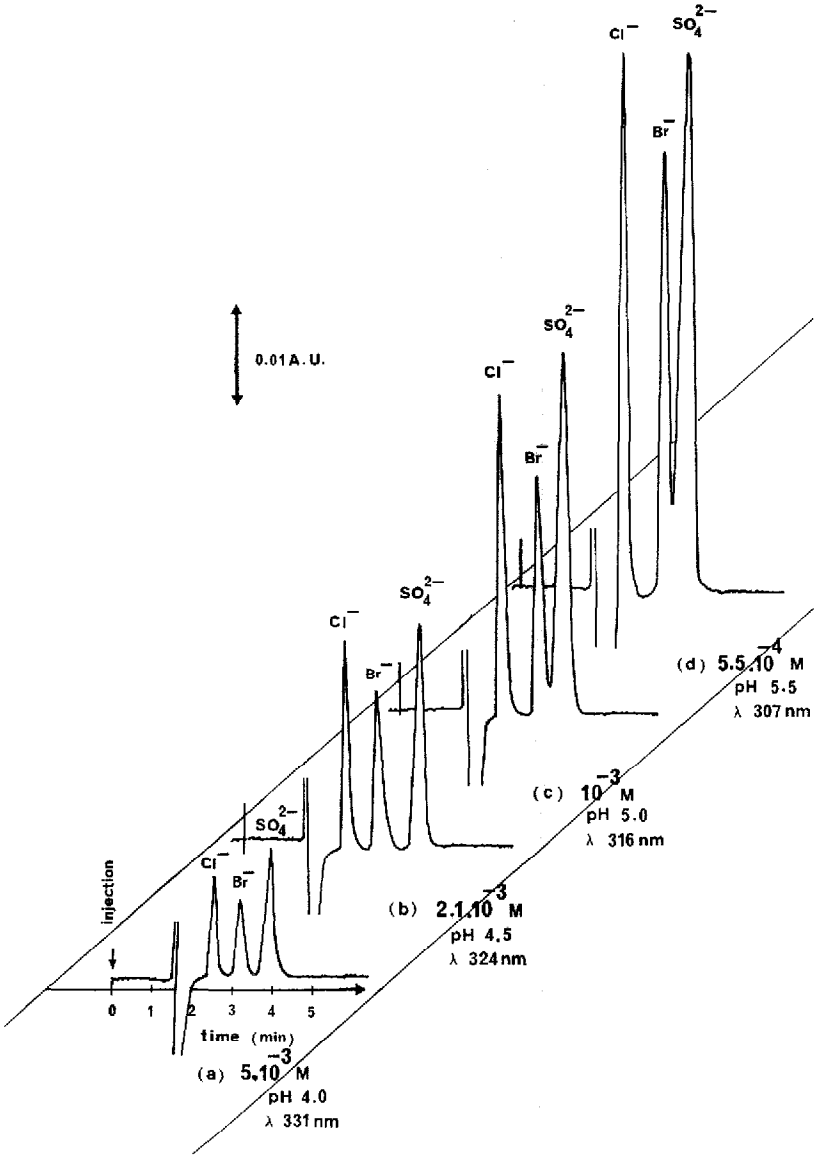

Fig. 4. Chromatograms of a mixture of Cl^-, Br^- and SO_4^{2-} carried out with four isocapacitive mobile phases having an initial absorbance of 0.6 A. Column, Ionospher A (Chrompack) (250 × 4.8 mm I.D.); eluent, pyromellitate buffer; flow-rate, 2 ml min^{-1}; injection volume, 100 μl; solute concentration, $4 \cdot 10^{-4}$ mol l^{-1} (14–38 ppm).

The fairly good agreement between the theoretical and observed slopes illustrated in Fig. 3 suggests that the solute elution is achieved by all eluent species (21.5% as H_2E^{2-}, 67.8% as HE^{3-} and 10.7% as E^{4-}), in proportion to their concentrations. This observation, despite the low probability of a multi-charged eluent ion interacting with three or more ion-exchange sites on a low-capacity exchanger, may be attributed to the macroporous resin structure (easy access to the sites on the walls of the pores) and to the acid–base equilibria. Moreover owing to the highly hydrophilic character of the mobile phase, and to the high charges on the eluting species, π–π interactions can be neglected with respect to the ion-exchange process.

Detection optimization and limits of detection

Several pyromellitate buffers give the same retention time for solutes bearing the same charge: these are isocapacitive eluents. However, these eluents are not equiv-

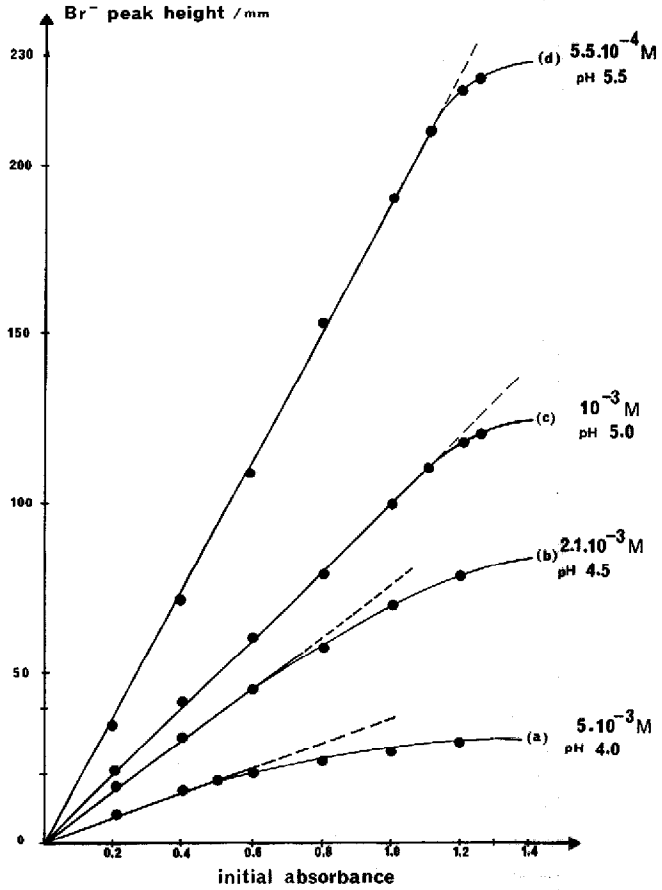

Fig. 5. Elution peak heights of Br^- *versus* the initial absorbance of the pyromellitate buffer for several concentration–pH combinations giving a constant retention for Br^-. Operating conditions as in Fig. 4 except solute concentration, 32 ppm.

alent as regards sensitivity. Fig. 4 illustrates a comparison between four isocapacitive eluents ($k'_{SO_4^{2-}} = 1.7$).

All the chromatograms are similar with regard to separation, except for slight variations due to changes in selectivity when modifying the pH. The variations in resolution observed between Br^- (univalent anion) and SO_4^{2-} (divalent anion) arise from the different slopes, $-x/y$, of the log k' *versus* log $[E^{y-}]$ plots for these ions as the eluent charge is altered according to the pH.

However, for all the solutes, the peaks are six times higher with mobile phase d than with a, which is about ten times more concentrated. Eqn. 5 predicts that the peak height should be proportional to the ratio ε_E^λ/y. This ratio was calculated to be 55, 113, 208, 337 for mobile phases a, b, c and d, respectively, and these values were in good agreement with the peak-height ratios in Fig. 4. It was apparent from UV absorbance spectra and absorbance measurements at various wavelengths and different pH values that ε_E^λ changes markedly with λ but only slightly with pH and therefore with y, within the wavelength range involved in the detection process; for example, the relative variation of ε_E^λ is less than 10% at $\lambda = 310$ nm, when y varies from 2.2 (pH 4.0) to 3.3 (pH 5.5). These observations are also illustrated in Fig. 6 (spectra c and d). As a result, a very low-concentration pyromellitate buffer, with a high apparent charge to balance the decrease in eluting power, is to be recommended.

Moreover, the sensitivity can be even better when the most dilute buffer is used. Fig. 5 shows the variations of the bromide peak height *vs.* the initial absorbance, fixed by the detection wavelength, all other conditions remaining the same. Not only does the slope increase as the buffer concentration decreases, owing to the factor ε_E^λ/y, but also the linearity range broadens.

This deviation from linearity occurs when the Lambert–Beer law is no longer obeyed, and generally has two origins: the concentration of the absorbing species is too high or the light is not strictly monochromatic.

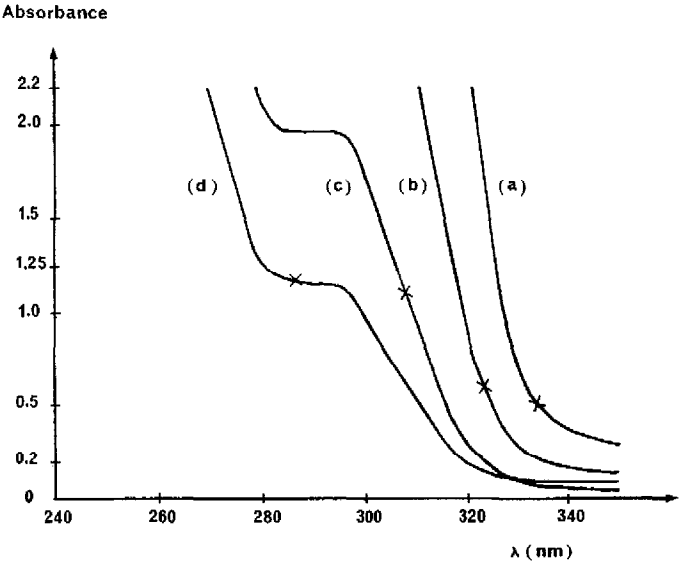

Fig. 6. UV spectra of the four pyromellitate buffers in Fig. 4.

TABLE I

DETECTION LIMITS OF SOME ANIONS

Column: 25 cm × 0.46 cm I.D. Stationary phase: Ionospher A (Chrompack). Mobile phase: $5.5 \cdot 10^{-4}$ *M* pyromellitate buffer (pH 5.5). Detection: UV at 285 nm; initial absorbance, 1.2 A. Flow-rate: 1 ml min^{-1}. Sensitivity: 0.0025 a.u.f.s. Injection: 100 μl.

Anion	*Capacity factor*	*Concentration (ppb)*	*Detection limit (amount injected)*	
			ng	*mole*
NO_2^-	0.62	51	5.1	0.11
NO_3^-	0.90	50	5.0	0.08
SO_4^{2-}	1.24	25	2.5	0.026

The advantage of the most dilute pyromellitate buffer is evident from the UV absorption spectra (Fig. 6). The crosses indicate the wavelength beyond which the deviation is occurring. The presence of a plateau is favourable from the point of view of monochromaticity defects or reproducibility.

Under optimum conditions, the detection limits, defined as the amount giving a signal-to-noise ratio of 3, are of the order of a few tens of ppb for an injection volume of 100 μl. Typical values are given in Table I.

Quantitative analysis

Fig. 7a and b show experimental calibration graphs obtained by measuring peak heights and peak areas, respectively. As predicted by eqns. 5 and 6, the plots

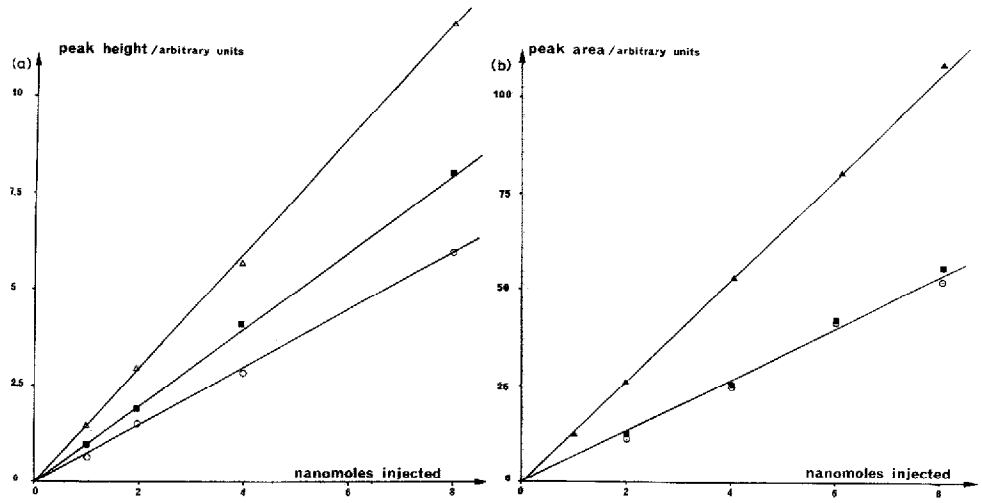

Fig. 7. Variation of (a) peak height and (b) peak area *versus* amount of solute injected (nanomoles). Column, PRP X-100 (Hamilton) (150 × 4.1 mm I.D.); eluent, pyromellitate buffer ($5 \cdot 10^{-4}$ mol l^{-1}; pH 4); flow-rate, 1 ml min^{-1}; injection volume, 20 μl; initial absorbance, 1.08 A (λ 300 nm). Solutes: ○, NO_3^-; ■, Br^-; △, Cl^-; ▲, SO_4^{2-}.

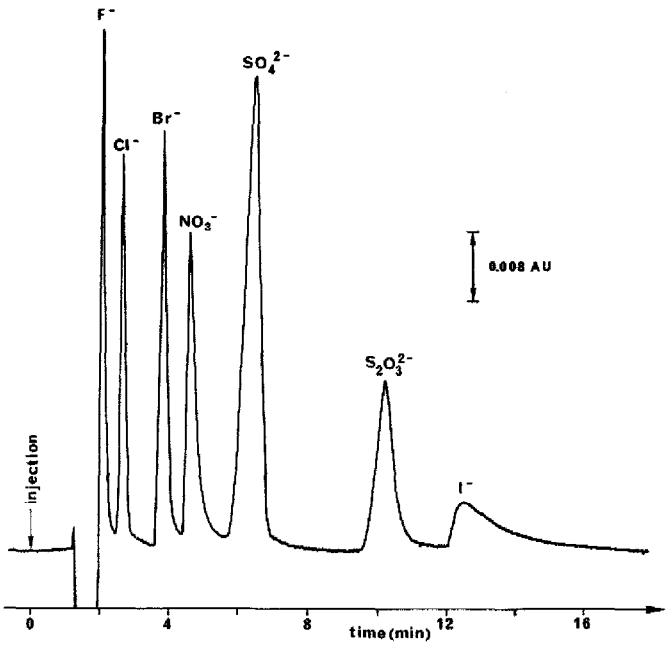

Fig. 8. Separation of some common inorganic anions. Operating conditions as in Fig. 7. Solute concentration: $4 \cdot 10^{-4}$ mol l^{-1} (7–50 ppm).

are linear in both instance and, for quantitation based on peak-area mesurements, the slope for divalent anions (SO_4^{2-}) is twice that for univalent anions, such as NO_3^- and Br^-.

Applications

A chromatogram obtained with the macroporous resin for some common inorganic anions is shown in Fig. 8. In spite of large differences in affinity, good resolution is observed within a reasonable time.

The determination of nitrate in drinking water is important in environmental problem and the analysis of Paris city water was taken as an example. Operating conditions were chosen in order to have a short analysis time (5 min), good sensitivity and good resolution between anions eluted in the vicinity of nitrate ($k' = 1.1$), *i.e.*, Cl^- ($k' = 0.5$) and SO_4^{2-} ($k' = 1.7$). The nitrate content of this sample was found to be 18.6 ppm from standard additions. Under these conditions (Chrompack Ionospher A column and pyromellitate buffer, $2.1 \cdot 10^{-3}$ mol/l, pH 4.5), nitrite ions are eluted between chloride and nitrate and consequently can be detected, if present, in the same run.

Taking advantage of the higher capacity of the ion exchangers used, small amounts of some ions can be detected in the presence of large amounts of other ions as the column is less easily overloaded.

Typical examples of applications involved the determination of bromide and nitrate in plant extracts in food chemistry. Much greater amounts of chloride and phosphate are generally present simultaneously. First an eluent was selected that gave

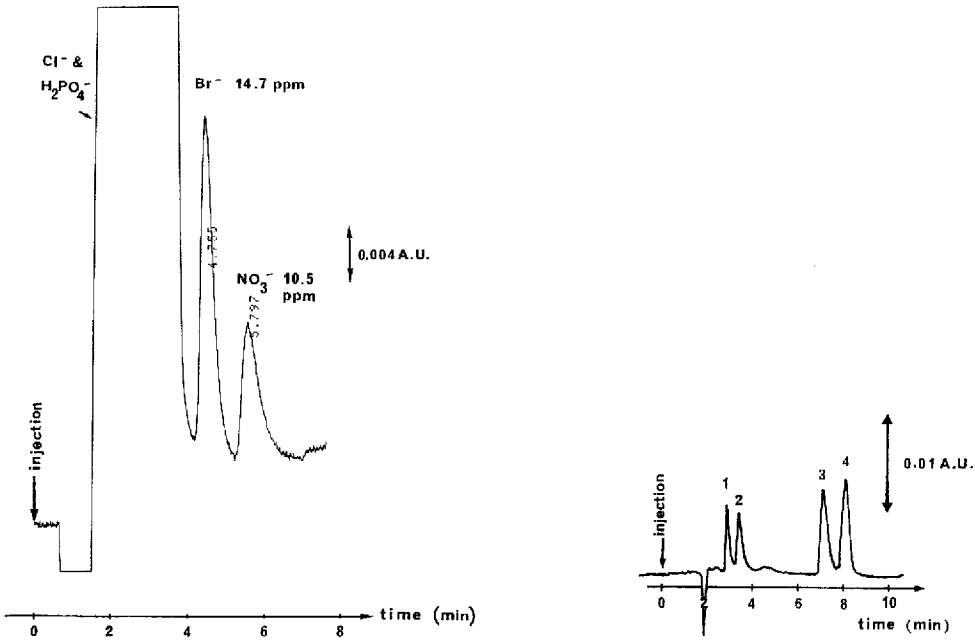

Fig. 9. Analysis of carrot extract. Column, PRP X-100 (Hamilton) (150 × 4.1 mm I.D.); eluent, pyromellitate buffer ($5 \cdot 10^{-4}$ mol l^{-1}; pH 3); flow-rate, 1 ml min^{-1}; injection volume, 20 μl; initial absorbance, 1.09 A (λ 295 nm).

Fig. 10. Analysis of unsaturated carboxylic acids. Column, Ionospher A (Chrompack) (250 × 4.8 mm I.D.); eluent, pyromellitate buffer ($3 \cdot 10^{-3}$ mol l^{-1}; pH 6.1); flow-rate, 2 ml min^{-1}; injection volume, 100 μl; initial absorbance, 0.5 A (λ 296 nm); solute concentration, 0.9–9.2 ppm. Solutes: 1 = acrylate; 2 = methacrylate; 3 = maleate; 4 = fumarate.

a good resolution between the early eluted anions. This eluent must have a low eluting power, but it is useful to adopt a concentration corresponding to the preceding plateau on the absorption spectrum. Therefore, the pH was lowered to 3, leading to an apparent charge close to 1.5. Using this mobile phase, the resolution between chloride and bromide is good enough to permit the detection of 3 ppm of Br^- in the presence of 1750 ppm of Cl^-. The ion chromatographic analysis of a carrot extract is shown in Fig. 9.

Pyromellitate buffers and indirect UV detection can also be applied to organic anions. As an example, Fig. 10 shows the separation of unsaturated carboxylic acids widely used as dienophilic reagents in organic synthesis.

CONCLUSION

Indirect photometric detection can easily be used in ion chromatography. The detectability is improved by appropriate selection of the mobile phase composition. It is important to seek an eluent ion that possesses both a high molar absorptivity and a convenient eluting power; pyromellitate buffers satisfy these two requirements. Under optimal operating conditions, the limit of detection of inorganic anions was

at the nanogram level. Indirect UV detection is growing in interest as a convenient detection mode in liquid chromatography and several recent papers have described its application to non-electrolytes[18–20].

ACKNOWLEDGEMENT

We thank M. Grenotton (Chrompack-France) for the gift of Ionospher A cartridges.

REFERENCES

1 D. T. Gjerde and J. S. Fritz, *Ion Chromatography*, Hüthig, Heidelberg, 2nd ed., 1987.
2 J. G. Tarter (Editor), *Ion Chromatography*, Marcel Dekker, New York, 1987.
3 J. Weiss, *Handbuch der Ionenchromatographie*, VCH, Weinheim, 1985.
4 J. S. Fritz, *Anal. Chem.*, 59 (1987) 335A.
5 H. Small, T. S. Stevens and W. L. Bauman, *Anal. Chem.*, 47 (1975) 1801.
6 T. S. Stevens, J. C. Davis and H. Small, *Anal. Chem.*, 53 (1981) 1488.
7 Y. Hanaoka, T. Murayama, S. Muramoto, T. Matsuura and A. Nanba, *J. Chromatogr.*, 239 (1982) 537.
8 G. O. Franklin, *Int. Lab.*, 15, No. 6 (1985) 56.
9 H. Shintani and P. K. Dasgupta, *Anal. Chem.*, 59 (1987) 802.
10 P. R. Haddad and A. L. Heckenberg, *J. Chromatogr.*, 300 (1984) 357.
11 T. H. Jupille and D. T. Gjerde, *J. Chromatogr. Sci.*, 24 (1986) 427.
12 D. T. Gjerde, *Int. J. Environ. Anal. Chem.*, 27 (1986) 289.
13 R. C. L. Foley and P. R. Haddad, *J. Chromatogr.*, 366 (1986) 13.
14 P. R. Haddad and C. E. Cowie, *J. Chromatogr.*, 303 (1984) 321.
15 A. Diop, A. Jardy, M. Caude and R. Rosset, *Analusis*, 14 (1986) 67.
16 A. Diop, A. Jardy, M. Caude and R. Rosset, *Analusis*, 15 (1987) 168.
17 R. E. Pauls, R. W. McCoy, E. R. Ziegel, T. Wolf, G. T. Fritz and D. M. Marmion, *J. Chromatogr. Sci.*, 24 (1986) 273.
18 G. Schill and J. Crommen, *Trends Anal. Chem.*, 6 (1987) 111.
19 T. Takeuchi and D. Ishii, *J. Chromatogr.*, 393 (1987) 419.
20 T. Takeuchi and D. Ishii, *J. Chromatogr.*, 396 (1987) 149.
21 R. Rosset, D. Bauer and J. Desbarres, *Chimie Analytique des Solutions et Microinformatique*, Masson, Paris, 1979.